Global Journal of Researches in Engineering
Electrical and Electronics Engineering
Volume 13 Issue 4 Version 1.0 Year 2013
Type: Double Blind Peer Reviewed International Research Journal
Publisher: Global Journals Inc. (USA)
Online ISSN: 2249-4596 & Print ISSN: 0975-5861

# Finger Typed Electrode Based Electro-Optical Demodulator Fabricated on High Resistivity Silicon

By Quazi Delwar Hossain, Gian-Franco Dalla Betta, Lucio Pancheri & David Stoppa

*Chittagong University of Engineering and Technology, Chittagong, Bangladesh*

*Abstract -* This paper focus on a finger typed electrode based electro-optical photo mixing demodulator. This device is fabricated on high resistivity silicon in custom technology. The main performance indicatorssuch as DC characteristics, DC and AC demodulation contrast and phase-linearity measurement of a test sample are experimentally characterized. Experimental results exhibit a good DC charge separation and good dynamic demodulation capabilities from 100Hz to 30MHz.The average linearity error of finger typed electrode device for square wave 4.09% has been measured. The dependency of the device performance on modulation frequency and voltage is also discussed.

*Keywords :* *electro-optical demodulator, high resistivity silicon, demodulation contrast, photonic device, modulation frequency.*

*GJRE-F Classification :* *FOR Code : 090606*


*Strictly as per the compliance and regulations of :*

# Finger Typed Electrode Based Electro-Optical Demodulator Fabricated on High Resistivity Silicon

Quazi Delwar Hossain [α], Gian-Franco Dalla Betta [σ], Lucio Pancheri [ρ] & David Stoppa [ω]

*Abstract -* This paper focus on a finger typed electrode based electro-optical photo mixing demodulator. This device is fabricated on high resistivity silicon in custom technology. The main performance indicatorssuch as DC characteristics, DC and AC demodulation contrast and phase-linearity measurement of a test sample are experimentally characterized. Experimental results exhibit a good DC charge separation and good dynamic demodulation capabilities from 100Hz to 30MHz.The average linearity error of finger typed electrode device for square wave 4.09% has been measured. The dependency of the device performance on modulation frequency and voltage is also discussed.

*Keywords : electro-optical demodulator, high resistivity silicon, demodulation contrast, photonic device, modulation frequency.*

## I. Introduction

Recently a lot of effort has been concentrated to develop standard 3D vision imagers due to the drastic increase in demand of 3D imaging system. The 2D-imaging system can evaluate only the intensity projection of a scene, there is no information about the depth of the 3D objects.

Range-imaging sensors acquire three-dimensional (3D) maps from a scene and can be used in a variety of applications such as bio medical appliances, surveillance system; several applications in automobiles, robomechatronics single point measurement etc. 3D image isextracting information from the geometric estimation of third co-ordinate of a scene.

In this work, we present a finger typed field assisted electro-optical demodulator fabricated in custom technology. After reviewing related research work in Section 2, the device architecture with its working principle and ISE-TCAD simulation are introduced in Section 3. In Section 4 the electro-optical characteristics of the device is reported. Finally the paper is concluded in Section 5.

*Author α : Faculty Member, Department of Electrical and Electronic Engineering, Chittagong University of Engineering and Technology, Chittagong, Bangladesh. E-mail : quazi@cuet.ac.bd*
*Author σ : Faculty Member, Department of Information Engineering and Computer Science, University of Trento, Trento, Italy.*
*Author ω : Senior Research Scientist, SOI Group, Fondazione Bruno Kessler, Trento, Italy.*

## II. Related Work

A number of applications that can detect the time or phase information of reflected light for 3D imaging are available in the literature. Depth information can be determined by correlating the incoming modulated light signal from the scene with a reference signal synchronous with the modulation signal of the light source [1]. In time-of-flight optical ranging, the phase information is used to plot the distance map of the observed scene, thus enabling the reconstruction of the shape and position of the observed objects [2]. TOF technique provides the best performance in terms of acquisition speed, reliability, overall cost of the system and is most suited to integrate electronic circuitry with more functionality. Several studies on image capturing techniques using specialized pixels coupled with active illumination have reported to produce images with information even at a low intensity level [3]-[4].TOF based 3D imagers so far reported in different literatures depending on the type of photo detector used in the pixels.

The time or phase information in addition to signal intensity is based on a variety of light-sensitivedevices such as: p-i-n photodiodes, linear or Geiger mode avalanche photodiodes and photomultipliertubes. Several works [5]-[8] reported a standard photodiode coupled with complex readout circuitry using indirect time-of-flight.

The key element of 3D range camera of photo demodulators have been implemented with different types of technologies such as: Charged Couple Device (CCD), Complementary Metal Oxide Semiconductor (CMOS) and CMOS/CCD hybrid approach. The photo generated charge is mixed on two or more photo-gates thus achieving an intrinsic demodulation effect [9]-[12].

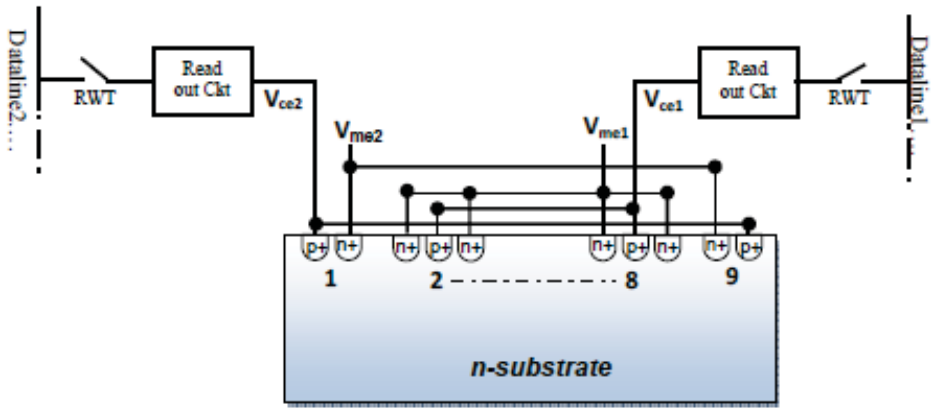


(a)

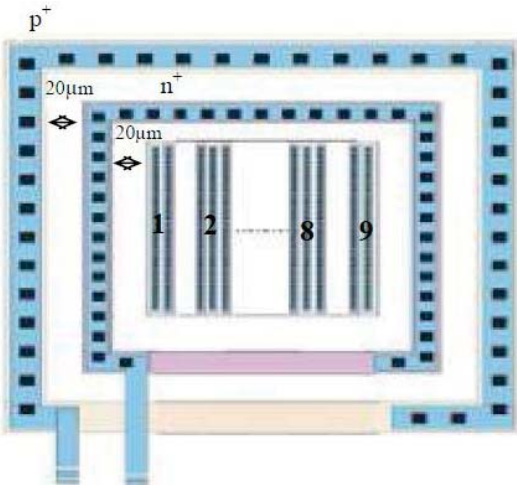


(b)

*Figure 1 :* (a) Cross sectional view of multiple strip CAPD and (b) Device layout

The advantage is the read-out channel simplicity which results in a small pixel size.The disadvantages are the lower sensitivity due to the presence of the "photo-gate", the lack of immunity to the ambient light and the cost of the non-standardtechnology.A Photonic Mixer Device (PMD) is an interesting solution for dynamic 3D-vision that is reported in [13]. An alternative demodulating detector structure, the Current Assisted Photonic Demodulator (CAPD) has been reported in [14].The function of detection and demodulation in a single device uses a modulated electric field that infiltrates deeper into the substrate to enhance the charge separation and collection mechanism.A linear Current Assisted Photonic Mixing Device fabricated on high resistivity silicon has been described in [15].

## III. Device Architecture and Working Principle

A finger-typed electrode based electro-optical demodulator consists of multiple strips. The cross sectional view and the layout of the device is shown in Figure 1 (a) and (b) respectively. The above Figure1(a) shows an active pixel that contains a finger typed photonic mixing demodulator that is integrated with a read out circuit and a row select transistor for each collecting electrode.This device has four electrodes, two of them known as collecting electrodes and connected to $V_{ce1}$ and $V_{ce2}$ and rest of them are known as modulating electrodes and connected to$V_{me1}$ and $V_{me2}$.These modulated electrodes are connected to the device substrate. This device consists of nine collecting electrodes. Among these electrodes, the seven central regions (from region 2 to region 8 as shown in Figure.01) consist of a p+ type detection junction and two n+ type substrate contacts. The rest of collection regions contain one collecting junction and one substrate contact, like the region 1 and 9 (Figure.1) [16].

All of the substrate contacts and the collection junctions are connected as shown in the device cross sectional diagram. The collecting electrode $V_{ce1}$ and the modulating electrode $V_{me1}$ are connected to the 2, 4, 6 and 8 regions according to the detection junctions and substrate contacts. On the other hand, the collecting electrode $V_{ce2}$ and the modulating electrode $V_{me2}$ are

connected to the region 1, 3, 5, 7 and 9 accordingly. This device is also enclosed with an n+ bulk-contact, shared along the array and placed at a minimum distance of about 20$\mu$m from the pixel boundary. A p+ ring is surrounded by n+ bulk-contact at a distance of about 20$\mu$m for better isolation of each device. The distance between the neighboring modulating electrodes is 20 $\mu$m and the total area of this device is 0.4mm × 0.4mm.Firstly, the device simulation software ISE-TCAD is used to investigate the operational behaviour of the device. In this device a potential difference is applied between the modulating electrodes to direct the signal charges towards the two detection regions.

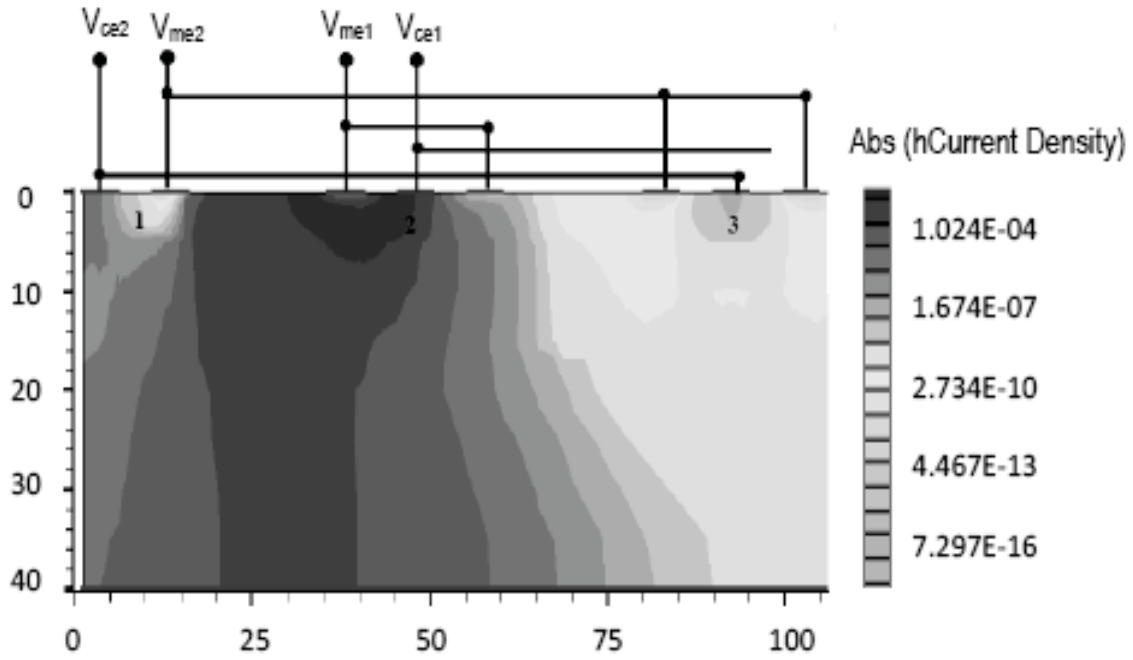


*Figure 2 :* Simulated hole current density under illumination

When a potential difference $\Delta V = V_{me2} - V_{me1}$ is applied at the modulated electrode $V_{me2}$. An electric field formed inside the substrate of the device guides the photo-generated charge carriers towards the detection electrode $V_{ce2}$.

At 780 nm light incident on the device surface the hole current density of this device shown in Figure 2. This simulated photograph shows the region 1and 2 according to the cross sectional view of the device shown in Figure 1(a). Most of the generated holes move toward the collecting electrode $V_{ce2}$, guided by the electric field with a voltage difference applied between two modulating electrodes i.e. $V_{me2} > V_{me1}$.

## IV. Performance Characteristics of the Device

The customize Fabricated structure is characterized electrically and optically. The demodulation contrast of the device and the effect of frequency and modulation voltage on it are assessed. Phase measurements are carried out to evaluate linearity of the device.

*a) Dc Characteristics*

An experimental characterization was carried out. The DC characterization set up of the test device is shown in above Figure 3.The device is enlightened with a wide spectrum lamp.

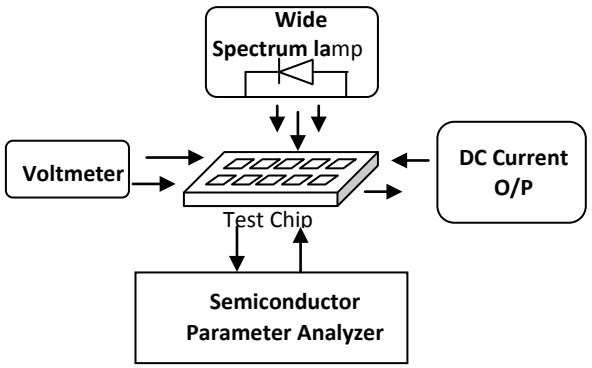


*Figure 3 :* Experimental setup for DC characterizations

In this measurement the required voltage at different electrodes can be supplied with a voltage source. A semiconductor parameter analyzer is used to read out the detection current from the collecting electrodes. Table: 1 shows the detection current from two collecting electrodes $I_{ce1}$ and $I_{ce2}$ at different modulation voltages.

*Table 1 :* Detection current at different modulation voltages

| $V_{me2}$(V) | $I_{ce1}$(μA) | $I_{ce2}$(μA) |
|---|---|---|
| 0.000 | 0.442 | 20.280 |
| 0.200 | 0.932 | 19.790 |
| 0.400 | 1.895 | 18.820 |
| 0.600 | 3.324 | 17.480 |
| 0.800 | 5.006 | 15.840 |
| 1.000 | 6.783 | 14.150 |
| 1.200 | 8.282 | 12.740 |
| 1.400 | 9.392 | 11.740 |
| 1.600 | 10.250 | 10.970 |
| 1.800 | 10.930 | 10.380 |

Now we can calculate the demodulation contrast by using the following equation.

$$DCDemodulationContrast(\%) = \left|\frac{I_{ce2} - I_{ce1}}{I_{ce2} + I_{ce1}}\right| \times 100\%$$

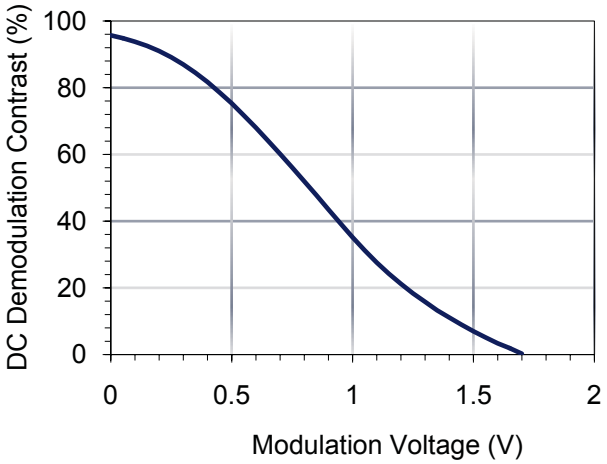


*Figure 4 :* Demodulation efficiency vs. Modulation Voltage

The device shows a maximum DC demodulation contrast larger than 90%, thus indicating that, this device is potentially enabling a very efficient mixing process.

*b) Dynamic Characteristics*

In order to measure average current at the collecting electrodes and the dynamic demodulation contrast we have conducted and experiment. The schematic representation of this experiment set up is shown in Figure 5.

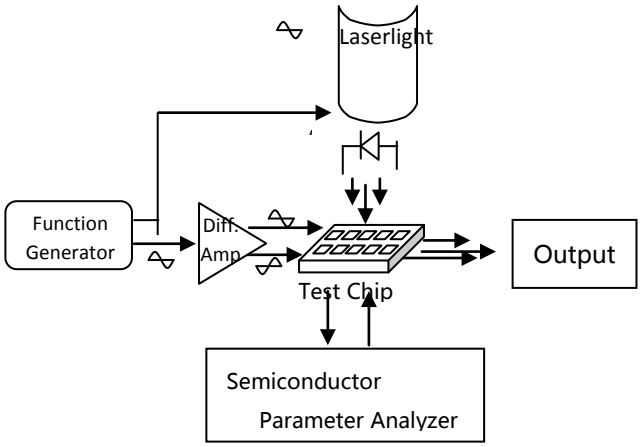


*Figure 5 :* Experimental setup for Dynamic characterizations

Two sinusoidal waves are generated by using a function generator. One of the two sinusoidal waves is used to modulate a laser emitter and illuminate the device. The other is connected to the input of a differential amplifier. The differential amplifier outputs with $180^0$ phase shift are connected to the modulating electrodes $V_{me1}$ and $V_{me2}$ of the device. The electric field formed in the substrate average current through the collecting electrodes $V_{ce1}$ and $V_{ce2}$ is read out with a Semiconductor Parameter Analyzer. For this measurement, the sinusoidal signal for laser emitter and two modulating signals are needed to use with an appropriate synchronization. At different modulation frequencies, the average current is measured under a 650nm red laser with 90% modulation depth used to illuminate the test device.The capability to separate and transfer the charges of a sensor to the corresponding output node can be expressed as a demodulation contrast. For data acquisition a LABVIEW software program was developed for the interface with PC and the experimental set-up.

The dynamic demodulation contrast is the most important performance indicator for this device. The demodulation contrast depends on both the amplitude of the modulation voltages and frequencies.

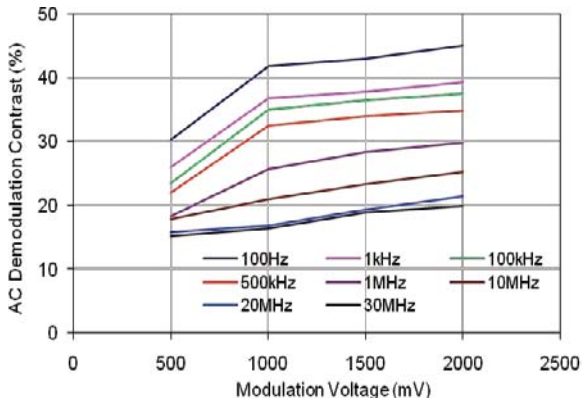


*Figure 6 :* Demodulation contrast at different modulation voltage

The dynamic demodulation contrast can be defined as:

$$\frac{I_{\max} - I_{\min}}{I_{\max} + I_{\min}} \times 100\ \% \quad \ldots\ldots\ldots\ldots\ldots (i)$$

Where $I_{max}$ and $I_{min}$ are the photo-generated currents flowing at collecting electrodes $V_{ce1}$ and $V_{ce2}$. The demodulation contrast for the finger typed device as a function of the modulation voltage amplitude at eight different frequencies from 100Hz to 30MHz is shown in Figure: 6.

By increasing the modulation voltage it should be possible to increase the majority current that cause the drift of the minority carriers, namely holes. When the modulation voltage is applied to the modulating electrodes, the photo generated holes arrive at the collecting electrode of the device. If applying more voltages, the electric field penetrates deeper in the substrate so that more holes reach detection node resulting in a higher demodulation contrast. Due to the larger voltage applying at the modulating electrodes the power consumption is increased. So the amplitude of modulation voltage should be carefully chosen. By increasing of the modulating frequency the decrease of the demodulation contrast can be described with respect to diffusion time. The photo-generated charges in the deeper of the substrate need more time to reach the active region where the demodulating electric field is present and thus reduces the demodulation contrast.

The phase linearity measurements performed between the applied phase and measured phase of the device. In these measurements a variable phase delay $\Delta V$ is applied between the laser input to illuminate the device and two modulation electrodes of the device. The value of $\Delta V$can be recovered acquiring four amplitude measurements with four different phase shifts $\phi_{11}$, $\phi_{12}$, $\phi_{21}$and $\phi_{22}$ applied to the modulated laser signal considered as -180°, -90°, 0° and +90° respectively [17]. The phase shift can be calculated with the equation (ii) given below:

$$\Delta\theta = \arctan\frac{I(\varphi_{11}) - I(\varphi_{21})}{I(\varphi_{12}) - I(\varphi_{22})} \quad \ldots\ldots\ldots\ldots (ii)$$

This measurement is performed using a sinusoidal wave and square wave modulation signals at 20 MHz, and the resulting phase is reported in Figure: 7 for this device. The average linearity error of finger typed electrode device for square wave is 4.09% thus, validating the good linearity of the device.

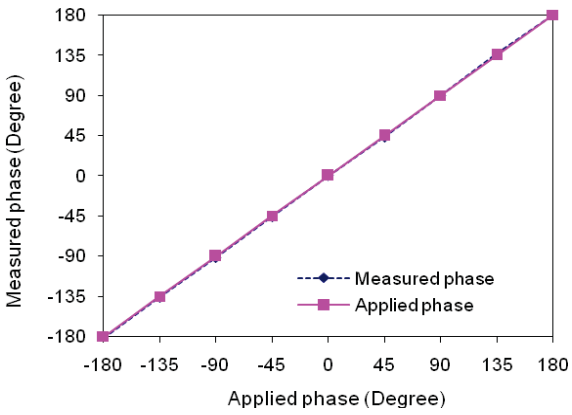


*Figure 7 :* Phase linearity measurement for Finger typed Device for Square wave

*c) Device Capacitance Measurement*

Figure: 8 is shown the experimental setup for capacitance measurement of this device. An LCR Meter is used to measure capacitance accurately. The LCR meter serves two main functions- measure the capacitance of the device and supply the required biasing voltage across the junction. This experiment is controlled by using a LABVIEW program via GPIB interface between the Computer and the LCR meter.

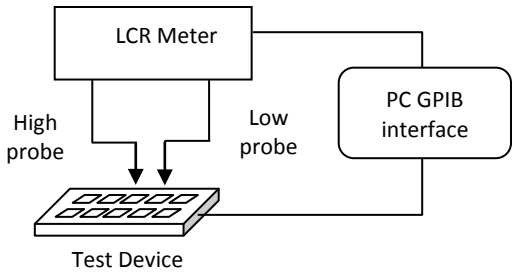


*Figure 8 :* Set-up for device capacitance measurement

At three different frequencies- 3MHz, 1 MHz and 100 kHz the C-V response of the device is shown in Figure: 9. Due to a larger depletion width the higher reverse bias produces a lower capacitance. At lower frequency, the capacitance is larger than at higher frequency. Because of their finite charging and discharging time the deep-level impurities in the space charge region make the capacitance to be frequency dependent [18, 19].

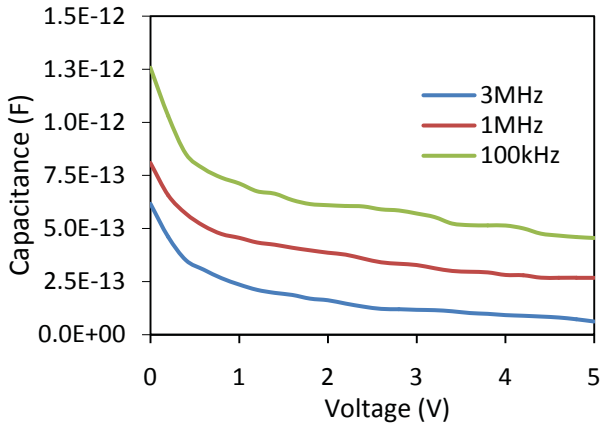


*Figure 9 :* C-V characteristics of the device

## V. Conclusion

This paper has described the characterization of a finger typed electro-optical demodulator fabricated in a custom technology on high resistivity silicon substrates. A 400µm × 400µm structure with finger typed electrodes has been considered and tested in terms of electrical and electro-optical performance. The maximum phase linearity error between the applied phase and the measured phase is 4.09% for square wave. In particular, the DC and dynamic demodulation performance of the multiple strip devices has been investigated. The measured dynamic demodulation contrast is more than 20% at 20 MHz modulation frequency. This customize device corresponds to understand field assisted photo mixing demodulator in term of optimizing the performance to make them in complementary metal-oxide-semiconductor technology.

## Acknowledgements

This work has been funded by "Netcarity" European Integrated Project (www.netcarity.org) and supported by the Fondazione Bruno Kessler (FBK), Trento, Italy.

## References Références Referencias

1. I.Moring, T.Heikkinem, R.Myllyla and A.Kilpela, "Acquisition of three dimensional image data by a scanning laser range finder" Opt.Eng. Vol.28 pp 897-905, 1989.
2. B. Jaehne, H. Haussecker and P. Geissler, Eds., "Handbook of Computer Vision and Applications. Vol. 1: Sensors and Imaging", Academic Press, San Diego, 1999.
3. S. Ando and A. Kimachi, "Time-Domain Correlation Image Sensor: First CMOS Realization of Demodulator Pixels Array", IEEE CCD/AIS Workshop, pp.33-36, Karuizawa, Japan, 1999.
4. J. Ohta, K. Yamamoto, T. Hirai, K. Kagawa and M. Nunoshita, "An Image Sensor with an In-Pixel Demodulation Function for Detecting the Intensity of a Modulated Light Signal", IEEE Trans. ED, vol.50, no.1, pp166-172, January 2003.
5. R.Jeremias, W.Brockherde, G.Doemens, B.Hosticka, L.List and P.Mengel, " A CMOS Photosensor Array for 3D Imaging Using Pulsed Laser", Proceedings of ISSCC'01, paper 16.5,Sanfransisco (CA) USA,Feb, 2001.
6. O .M. Schrey, 0. Elkhalili, P. Mengel', M. Petermann, W. Brockherde, B.J. Hosticka "A 4x64 Pixel CMOS Image Sensor for 3D Measurement Applications" , IEEE Journal of Solid State Circuits, vol.39, no.7, pp.1208-1212, July, 2004.
7. David Stoppa, Luigi Viarani, Andrea Simoni, Lorenzo Gonzo, MattiaMalfatti, GianmariaPedretti, "A 16x16-Pixel Range-Finding CMOS Image Sensor" Proceedings of IEEE European Solid-State Circuits Conference- ESSCIRC'04, pp. 419-422, September, 2004.
8. D.Stoppa, L.Viarani, A.Simoni, L.Gonzo, M.Malfatti, G.Pedretti " A 50×30 pixel CMOS sensor for TOF-based real time 3D imaging" proceedings of the IEEE workshop on CCD and advanced Image sensors, pp.230-233,2005.
9. R.lange and P. Seitz, "Solid- State Time-of-Flight Camera", IEEE Journal of Quantum Electronics, Vol.37,no.3, pp. 390-397, March 2001.
10. R. Miyagawa and T. Kanade, "CCD-Based Range-Finding Sensor", IEEE Trans. ED, vol.44, no.10, pp.1648-1652, 1997.
11. T. Oggier, M. Lehmann, R.Kaufmann, M. Schweizer, M. Richter, P. Metzler, G.Lang, F. Lustenberger, N. Blanc,"An all solid-state optical range camera for 3D real-time imaging with sub-centimeter depth-resolution(SwissRanger), Proceeding of SPIE Vol.5249, pp. 634-645, 2003.
12. Mesa Imaging website: http: www.swissranger.ch
13. Rudolf Schwarte, "Dynamic 3D Vision", Proceedings of International Symposium on Electron Devices for Microwave and Optoelectronic Applications, pp.241-248, 15-16 November, 2001.
14. Van Nieuwenhove, W.VanDerTempel and M.Kuijik, "Novel Standard Detector using majority for guiding Photo-Generated Electrons towards Detecting Junctions", Proceedings Symposium IEEE/LEOS Benelux Chapter, pp.229-232, 2005.
15. L. Pancheri, D. Stoppa, N. Massari, M. Malfatti, C. Piemonte, G.-F. DallaBetta, "Current Assisted Photonic Mixing Devices Fabricated on High Resistivity Silicon" Sensor Conference, 2008 IEEE, ISSN: 1930-0395, E-ISBN: 978-1-4244-2581-5, Print ISBN: 978-1-4244-2580-8, Page: 981 - 983 26-29 October. 2008.
16. Quazi Delwar Hossain,Gian-Franco Dalla Betta, Lucio Pancheri, David Stoppa, Sagar Kumar Dhar, "Multiple Strip Photo Mixing Demodulator for 3D Imaging Implemented on High Resistivity Silicon" Proceedings of 7th International Conference on

Electrical and Computer Engineering, 20-22 December, 2012, Dhaka, Bangladesh, Page 430-433.
17. R. Lange, P. Seitz, A. Biber and R. Schwarte. “Time-of Flight Range Imaging with a Custom Solid State Image Sensor”, *EOS/SPIE International Symposium*. Munich, Germany, June 14-18 1999, pp. 180-191.
18. D. K. Schroder, *Semiconductor material and device characterization*, 2nd ed. New York: Wiley, 1998.
19. C. F. Robinson, "Micro probe analysis," 1973.

This page is intentionally left blank